Lead Article

Acta Cryst. (1991). A47, 453-469

Crystallography and Structural Phase Transitions, an Introduction*

By Ekhard K. H. Salje

Department of Earth Sciences and Interdisciplinary Research, Centre for Superconductivity, University of Cambridge, Downing Street, Cambridge CB2 3EQ, England

(*Received* 29 *October* 1990; *accepted* 9 *May* 1991)

Abstract

Structural phase transitions which involve the generation of lattice strain (*i.e.* in ferroelastic and co-elastic crystals) are reviewed. Landau-Ginzburg theory is found to lead to an appropriate description of order parameters following the theoretical predictions over large temperature intervals. A quantum extension of Landau-Ginzburg theory is presented which describes the saturation of order parameters at low temperatures. Coupling between different order parameters is relevant if more than one phase transition (or lattice instability) occurs in a crystal. Finally, the importance of microstructures and kinetic processes for the structural behaviour of crystals is pointed out.

1. Introduction

Crystal structures change as a function of temperature, pressure, chemical replacement and other thermodynamic parameters. These changes can be straightforward to understand, as may be illustrated for simple structures such as NaCl where interatomic distances and thermal ellipsoids increase with increasing temperature until the thermal energy suffices to produce defects and, ultimately, leads to melting. This 'standard' behaviour is in contrast with the evolution of crystal structures which contain inherent degrees of freedom which are activated when the external conditions of the crystal are changed. One of the simplest examples is the perovskite structure and its derivatives. At sufficiently low temperatures, these structures tend to have low symmetry with substantial distortions and tilts of the octahedral complexes, cation positions shifted away from the centres of the coordination polyhedra and so forth (Fig. 1). The increase of temperature changes these distortions until some of them disappear. Further heating does not then lead to a reappearance of these particular distortions - once they are annihilated they may only reappear if the crystal is recooled to its former conditions. It is convenient then to distinguish between the distorted crystal structure and the undistorted crystal structure as two phases. The transition between them, as generated by temperature, pressure or any other thermodynamic variable, is called a structural phase transition.

The investigation of such structural phase transitions in their various guises - including cation or molecular ordering, various types of distortions, polytypism to name but a few - may have remained of limited interest to a small group of crystallographers were it not for two surprising effects. Firstly, it was found that all phase transitions observed in crystals follow a similar pattern once they are described in the appropriate physical parameters. This discovery led to the definition of the 'order parameter' as the all-important physical quantity describing the phase transition. We shall see below how this quantity can be defined.

Secondly, inspection of the macroscopic physical behaviour of crystals showed that effects such as extreme softness, mechanical switching of domains, large dielectric constants, ferroelectricity and many other effects of great value for the application of crystals as device materials are closely related to

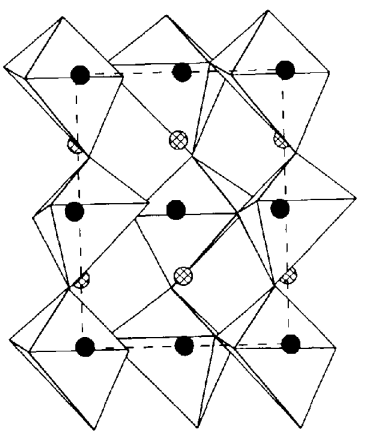

Fig. 1. Crystal structure of NH_4IO_3 at room temperature. The typical distortions of a perovskite structure are well developed here: the octahedra are tilted, the central octahedral cation and the NH_4 group are off centre and the oxygen coordination around iodine is distorted (data after Bismayer *et al.*, 1979; Salje, 1989).

* *Editorial note*: This invited paper is one of a series of comprehensive Lead Articles which the Editors invite from time to time on subjects considered to be timely for such treatment.

0108-7673/91/050453-17$03.00

structural phase transitions and, indeed, in most cases they are a direct consequence of such phase transitions.

The fascination with these two aspects of phase transitions, namely the generality of the transition behaviour and the extreme physical properties which accompany the transition, has attracted many able physicists and crystallographers over the last decades. They created a mature and widely extended research subject which the author will not be able to review in any detail (*e.g.* see Bruce & Cowley, 1981; Salje, 1990*a*). He rather enjoys a frankly partisan view and will concentrate on particular recent developments both on the experimental and the somewhat theoretical side. References are given so that the reader can enhance and complete the picture.

2. The order parameter

Let the phase transition occur between two structures with different space groups. In order to obtain the closest possible connection between the two phases we shall also require that all symmetry elements of the low-symmetry phase are already present in the high-symmetry form, *i.e.* the space group of the low-symmetry form is a subgroup of the high-symmetry space group. In order to understand the transition process the primary task is to identify the process of symmetry breaking. This can happen in various ways. Imagine a mirror plane in the yz plane as the critical symmetry element and the symmetry-related positions xyz and $\bar{x}yz$. The symmetry breaking can now be due to a shift of both positions parallel to the x axis by δx. The new coordinates are $x+\delta x, y, z$ and $\bar{x}+\delta x, y, z$ so that the mirror plane is destroyed. One would generally call such a transition mechanism 'displacive' although a strict definition of a displacive transition in such simple geometrical terms is, in fact, only useful if the translational symmetry is unaffected by the phase transition (which is rarely the case). A more appropriate definition of the term displacive will be discussed later.

Another mechanism by which the mirror symmetry can be broken is by different occupancies of the two positions, *e.g.* by ordering of cations such as Al and Si in aluminium silicates. This transition would be of the 'order/disorder' type although it is clear that lattice relaxations due to the ordering process will inevitably lead to additional 'displacive' deformations. If the two positions are occupied by molecules which change their mutual orientation during the phase transition, the transition is normally called 'molecular order/disorder' type. Again, the lattice relaxations are normally rather large due to strong rotation–translation coupling (Dove, 1990; Lynden-Bell, Ferrario, McDonald & Salje, 1989). Influences from the partial or total localization of electronic wavefunctions leads to Anderson or Mott transitions and their periodic coupling with the lattice distortion destroys the translational symmetry and leads to Peierls transitions. Symmetry reduction due to spin degrees of freedom are relevant in ferro- and antiferromagnetic transitions. Many other types of transitions exist including mixtures between the above-mentioned main types.

Although there are many different ways in which a symmetry is broken, the common feature is always that a new variable exists which quantifies how far the system deviates from the high-symmetry form and in which direction (*e.g.* 'right' and 'left' must be identical in the vertical mirror plane but not when the mirror plane is destroyed). We can now fall back on the general principles of thermodynamics and define a quantity which specifies the thermodynamic state of the low-symmetry phase as the order parameter Q. The reduction of a crystallographic problem to thermodynamics has the great advantage that general solutions can be worked out which are independent of the individual crystal structure and therefore universal. Once these solutions are understood they can be reapplied to the problem in hand and help to identify the transition mechanism. Roughly speaking, the order parameter can be envisaged as follows: let $\rho_0(r)$ be the density function of the high-symmetry form and $\rho(r)$ that for the low-symmetry form at the most extreme degree of deviation from the high-symmetry form (*e.g.* at absolute zero temperature in most cases). The phase transition is then described by the difference between the two density functions called $\Delta\rho(r, T, P, N, \dots)$, for all intermediate thermodynamic conditions. The basic assumption for current theories of phase transitions is that this density function can be split into two factors

$$\Delta\rho(r, T, \dots) = Q(T, \dots)\Delta\rho(r)$$

where $\Delta\rho(r)$ is the difference between $\rho(r)$ and the extrapolated value of $\rho_0(r)$ for the same thermodynamic conditions under which $\rho(r)$ is measured (*e.g.* at 0 K) and Q is the order parameter. We have now separated the thermodynamic amplitude function Q, which is independent of all the crystallographic properties and totally universal, and the crystallographic features, which are summarized in $\Delta\rho(r)$. This approach predicts that the structural deformation pattern, including changes of atomic positions, occupancies, spin orientations *etc.*, once adopted during a phase transition, does not subsequently change. The only quantity which changes is the amplitude of this pattern, *i.e.* the order parameter. The essentials of the phase transitions are, thus, described by the order parameter Q. We shall see later how this concept has sometimes to be modified by the consideration of various interacting order parameters; the general concept remains valid even in those cases, however.

The correlation between the changes in the crystal structure due to a phase transition and the order

parameter leads to stringent symmetry constraints which allow us to work out which structural parameter can be affected and how. The order parameter breaks a particular symmetry which exists in the high-symmetry form but which does not exist in the low-symmetry form. This defines the transformation behaviour of the order parameter, given by the active representation of the high-symmetry space group. As the density function has the same transformation properties as the order parameter, we can also work out which structural changes are compatible with the symmetry of the order parameter. Only these structural changes are expected to occur during the structural phase transition. Structural analysis work allows us then to verify whether or not the order parameter has been chosen correctly and, *vice versa*, group theory predicts which coordinates, occupancies *etc.* are involved in the transition mechanism. The latter step can be of great help when the actual crystal structure of the low-symmetry phase is being solved. The relevant symmetry concepts have been worked out in great detail; they are one of the main working tools in the field of structural phase transitions (*e.g.* Toledano & Toledano 1980, 1982; Stokes & Hatch, 1988; Hatch, Artman & Boerio-Goates, 1990; Salje, 1990*a*).

We now return to the thermodynamic argument which says that by breaking the symmetry the order parameter Q is created as a new thermodynamic variable. This variable is necessary to specify the thermodynamic state completely. Under certain thermodynamic conditions, the low-symmetry phase will be more stable than the high-symmetry phase. The difference of the Gibbs energy which stabilizes the low-symmetry phase is called the excess Gibbs free energy G, which now depends on the thermodynamic parameters temperature T, pressure P, chemical composition N *etc.* and the order parameter Q:

$$G = G(T, P, N, \ldots, Q).$$

We can obtain the Gibbs energy $G(T, P, N, \ldots)$ that we observe under equilibrium conditions by using the minimum principle:

$$dG/dQ = 0.$$

There is always one trivial solution to the problem which is

$$G(T, P, N, \ldots) = 0$$

for one phase. This phase is taken for convenience as the high-symmetry phase and all quantities are measured with respect to this phase as excess quantities. We shall now derive some simple expressions for the excess Gibbs energy in the low-symmetry phase.

3. A simple structural model and its mean-field approximation

Let us consider the lattice instability along a specific direction in the reciprocal lattice. All lattice planes perpendicular to this direction are projected on this one-dimensional subspace, each plane marking a point in a chain. Each point is then characterized by an effective local potential and collective interactions between the points. The points are numbered l and the total potential can be written in terms of the local normal coordinates Q_l and conjugate momenta P_l. The equivalent Hamiltonian is

$$H = \sum_l [(1/2M)P_l^2 + \tfrac{1}{2}M\Omega_0^2 Q_l^2 + \tfrac{1}{4}uQ_l^4 + \ldots] - \tfrac{1}{2}\sum_{l \neq l'} v_{ll'} Q_l Q_{l'}.$$

Here, M is the effective mass, Ω_0 is the local frequency for small oscillations in the absense of interactions, u gives the strength of the anharmonicity (which is restricted to fourth order in this case) and $v_{ll'}$ are interaction constants.

The type of transition is now determined by the wavevector q_0 at which the Fourier transform of the interaction assumes its maximum value. The mean-field approximation of this Hamiltonian has been discussed in detail by Salje, Wruck & Thomas (1991) and the author will follow their arguments closely. The temperature dependence of the order parameter results from the dissipation-fluctuation theorem which links the variance of the order parameter $\sigma = \langle (Q_l - \langle Q_l \rangle)^2 \rangle$ with the excitation frequency Ω *via*

$$\sigma = (\hbar/2M\Omega) \coth (\hbar\Omega/2k_BT)$$

leading to the expectation values

$$\langle P_l^2 \rangle = (M\Omega)^2\sigma$$
$$\langle Q_l^2 \rangle = Q^2 + \sigma$$
$$\langle Q_l^4 \rangle = Q^4 + 6Q^2\sigma + 3\sigma^2.$$

The Gibbs free energy becomes

$$G = N\{\tfrac{1}{2}(M\Omega_0^2 - v + 3u\sigma)Q^2 + \tfrac{1}{4}uQ^4 + \tfrac{1}{2}M\Omega_0^2\sigma + \tfrac{3}{4}u\sigma^2 - \tfrac{1}{4}\hbar\Omega \coth (\hbar\Omega/2k_BT) + k_BT \ln [2 \sinh (\hbar\Omega/2k_BT)]\}.$$

Minimizing with respect to Q and Ω yields the mean-field equations:

$$(M\Omega_0^2 - v + 3u\sigma + uQ^2)Q = 0.$$
$$M\Omega^2 = M\Omega_0^2 + 3u(\sigma + Q^2).$$

The variance at the critical point is found by letting Q go to zero:

$$\sigma_c = (v - M\Omega_0^2)/3u$$

and for the order parameter in the low-symmetry

phase one obtains

$$Q^2 = 3(\sigma_c - \sigma).$$

The self-consistency condition for σ is

$$\sigma = \sigma_c(\eta\Omega_0/\Omega)\coth(\eta\Omega/\Omega_0 x)$$
$$\Omega^2 = \Omega_0^2[1 + \Delta(3 - 2\sigma/\sigma_c)]$$

where the normalized temperature x has been introduced as

$$x = k_B T/M\Omega_0^2\sigma_c.$$

The dimensionless parameter

$$\Delta = v/M\Omega_0^2 - 1$$

is proportional to the distance from the displacive limit with $v = M\Omega_0^2$ and

$$\eta = \hbar/2M\Omega_0\sigma_c$$

is a measure of the quantum influence at low temperatures. The quantum-mechanical fluctuation enhancements have an important influence on the system because the zero-point fluctuations with variance σ_s reduce the order parameter Q_s at zero temperature, as compared to its classical value Q_0 ($=3\sigma_c^2$) by

$$Q_s^2/Q_0^2 = 1 - \sigma_s/\sigma_c.$$

The value of σ_s is determined by the solution of the equation

$$(\sigma_s/\sigma_c)[1 + \Delta(3 - 2\sigma_s/\sigma_c)]^{1/2} = \eta$$

which follows from the self-consistency equation in the limit $T = 0$K. Simultaneously, the quantum fluctuations reduce T_c by

$$\frac{T_c}{T_c^{\text{class}}} = \frac{\eta/(1+\Delta)^{1/2}}{\operatorname{arctanh}[\eta/(1+\Delta)^{1/2}]}.$$

So far the phase transition has been assumed to be second order and higher-order anharmonicities of Q_l were ignored. Salje, Wruck & Thomas (1991) have shown that similar arguments hold in the displacive limit for a Hamiltonian including a sixth-order term. If the sixth-order term is present but the fourth-order term vanishes, one finds a classical tricritical phase transition.

The temperature dependence of the order parameter obtained by numerical solutions for $\sigma(T)$ is displayed in Fig. 2 for systems close to the displacive limit ($\Delta \ll 1$) and in Fig. 3 for $\Delta = 0{\cdot}2$. Comparison with experimental data in Fig. 4 shows quantitative agreement for values of $\Delta \ll 1$. In Fig. 5, the experimentally determined temperature dependencies of the structural order parameters in $LaAlO_3$, $Ca_{0{\cdot}98}Na_{0{\cdot}02}Al_{1{\cdot}98}Si_{2{\cdot}02}O_8$ and $Pb_3(PO_4)_2$ are shown with the theoretical curve for $\Delta \ll 1$. The square of the order parameter is plotted in the case of a second-order phase transition, whereas the fourth power is shown for the latter two compounds which are under (nearly) tricritical phase transitions. The agreement between the observations and the mean-field solutions is very good.

The classical Landau potentials follow now as the high-temperature approximations of the Gibbs free energies developed so far. Salje, Wruck & Thomas (1991) have shown that in the displacive limit (for which Landau theory is applicable) the Gibbs free energy becomes

$$G(T, Q) = G_0(T) + \tfrac{3}{2}[\sigma(T) - \sigma_c]uQ^2 + \tfrac{1}{4}uQ^4 + \tfrac{1}{6}cQ^6$$

where the mean-square fluctuations are given by

$$\sigma(T) = (k_B\Theta_s/M\Omega_0^2)\coth(\Theta_s/T)$$

in terms of the characteristic temperature $\Theta_s = 2T_s$

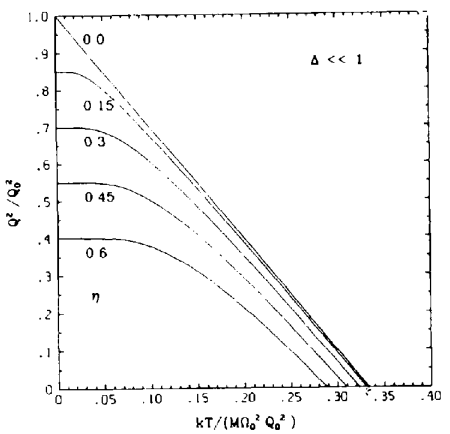

(a)

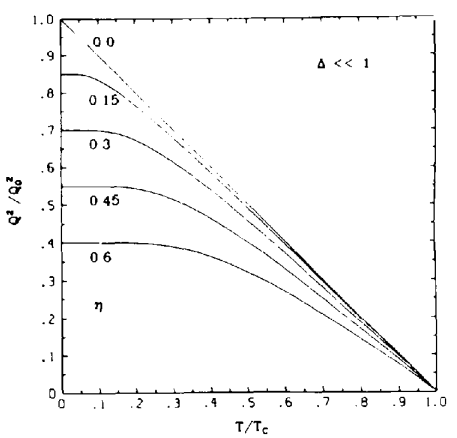

(b)

Fig. 2. (*a*) Calculated temperature dependence of the order parameter close to the displacive limit, $\Delta \ll 1$, for various values of the saturation parameter $\eta = 3\hbar/(2M\Omega_0 Q_0^2)$. (*b*) Same curves as in (*a*) but the temperatures are normalized with respect to the transition temperature T_c (from Salje *et al.*, 1991).

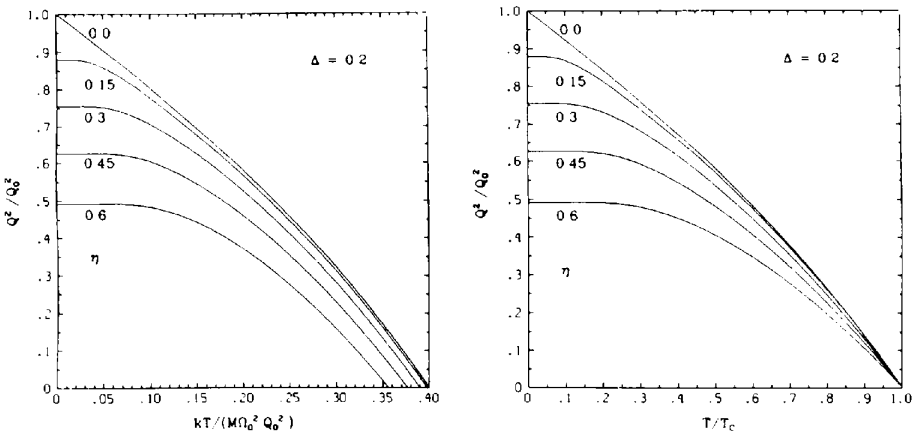

Fig. 3. Temperature evolution of the order parameter for $\Delta = 0{\cdot}2$. Same saturation parameters as in Fig. 2 (from Salje *et al.*, 1991).

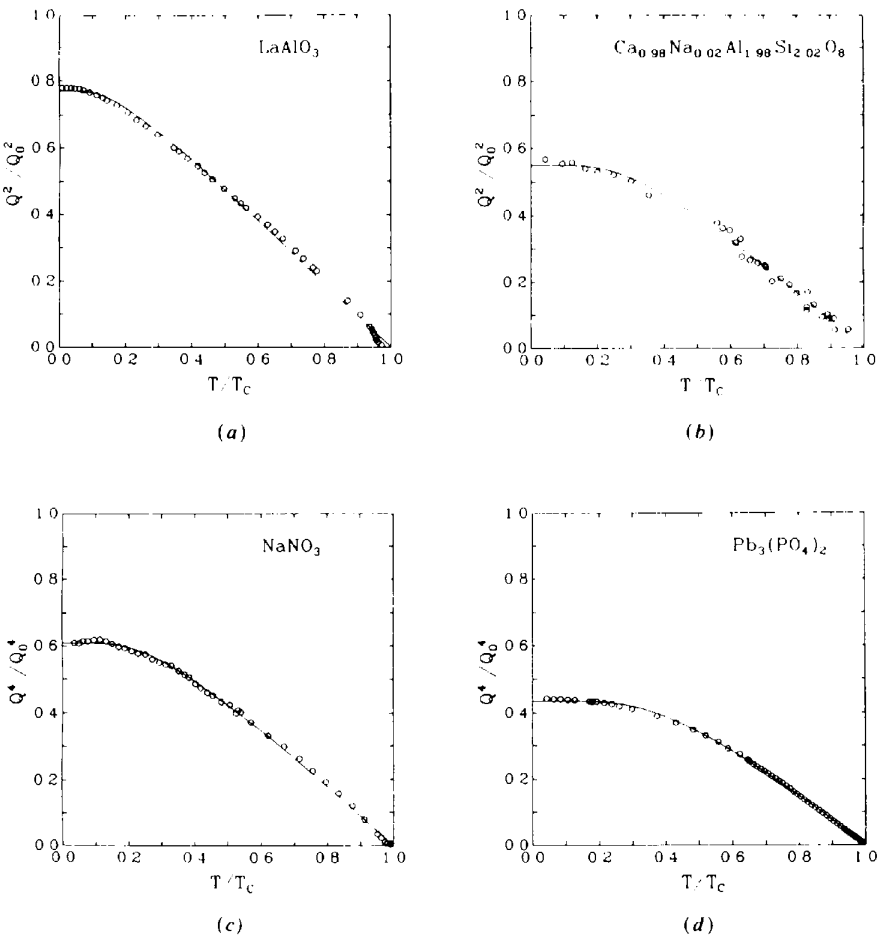

Fig. 4. Comparison of experimental data (circles) and theoretical predictions (lines) for the temperature dependence of the order parameter close to the displacive limit, $\Delta \ll 1$, for four representative cases:
$n = 2$ for second-order transitions: (*a*) $LaAlO_3$: $\Theta_s = 194{\cdot}1$ K, $\Theta_s/T_c = 0{\cdot}2345$; (*b*) $Ca_{0{\cdot}98}Na_{0{\cdot}02}Al_{1{\cdot}98}Si_{2{\cdot}02}O_8$: $\Theta_s = 264{\cdot}8$ K, $\Theta_s/T_c = 0{\cdot}4869$; $n = 4$ for tricritical phase transitions: (*c*) $NaNO_3$: $\Theta_s = 232{\cdot}9$ K, $\Theta_s/T_c = 0{\cdot}4131$; (*d*) $Pb_3(PO_4)_2$: $\Theta_s = 292{\cdot}3$ K, $\Theta_s/T_c = 0{\cdot}6393$, the parameters Θ_s and Θ_s/T_c were determined by least-squares refinement (from Salje *et al.*, 1991).

defined by

$$k_B\Theta_s = \tfrac{1}{2}\hbar\Omega_0$$

With the parameters $A = 3uk_B/m\Omega_0^2$, $B = u$ and the critical temperature T_c defined by

$$\Theta_s \coth(\Theta_s/T_c) = \tfrac{1}{3}M\Omega_0^2Q_0^2/k_B$$

the Landau potential becomes in its general form

$$G(Q, T) = G_0(T) + \tfrac{1}{2}A\Theta_s[\coth(\Theta_s/T) - \coth(\Theta_s/T_c)]Q^2 + \tfrac{1}{4}BQ^4 + \ldots.$$

In the high-temperature approximation ($T \gg T_s$) this equation yields

$$G(T, Q) = L(T, Q) = \tfrac{1}{2}A(T - T_c)Q^2 + \tfrac{1}{4}BQ^4 + \tfrac{1}{6}cQ^6.$$

Symmetry constraints are irrelevant in the model presented here. More complex Landau potentials appear in the case of multidimensional order parameters discussed in detail by Toledano & Toledano (1980, 1982), Stokes & Hatch (1988), Salje (1990*a*), Ishibashi, Hara & Sawada (1988) and many other authors; however, the underlying physical picture remains the same.

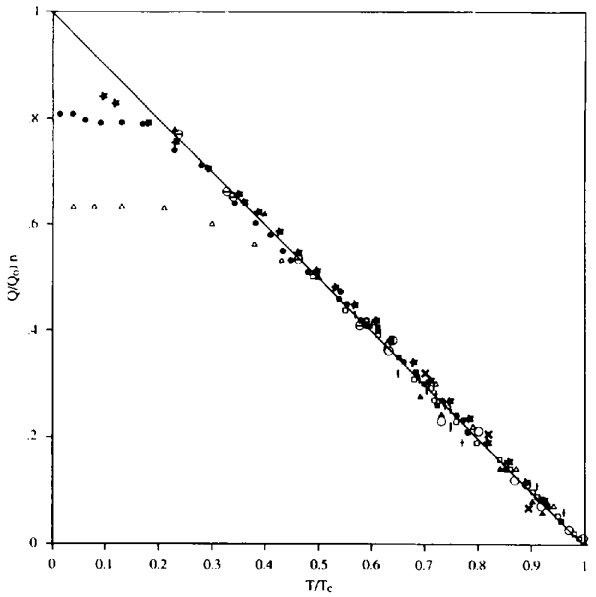

Fig. 5. Temperature evolution of structural order parameters Q to the power of n for some (nearly) second-order and tricritical phase transitions. The temperature is normalized with respect to T_c and the order parameter with respect to the extrapolated value at zero temperature, Q_c. $n = 2$ for second-order transitions: full circles: $LaAlO_3$ ($T_c = 800$ K); open circles: $Na_{0.69}K_{0.31}AlSi_3O_8$ ($T_c = 416$ K); circles with horizontal bar: $NaAlSi_3O_8$ ($T_c = 1251$ K); stars: SiO_2 ($T_c = 847$ K); open squares: As_2O_5 ($T_c = 578$ K); full squares: $Pb_3(AsO_4)_2$ ($T_c = 560$ K); open triangles: $Pb_3(PO_4)_2$ ($T_c = 455$ K); $n = 4$ for tricritical phase transitions: full triangles: $CaCO_3$ ($T_c = 1250$ K) [12]; dots with vertical bar: $CaAl_2Si_2O_8$ ($T_c = 513$ K) [13].

4. On the role of lattice parameters – the spontaneous strain

One of the most common features of many structural phase transitions is that the lattice parameters of a crystal change as a non-linear function of temperature, pressure or chemical composition. The dominant physical parameter which is needed to quantify such changes is the spontaneous strain which will now be introduced and, indeed, much of what can be concluded from precise measurements of the lattice parameters sometimes suffices to determine the order-parameter behaviour without the need for further structural information.

The spontaneous strain is the amount of strain which relates the low-symmetry form to the high-symmetry structure. Before the strain parameters are formally defined, we consider an instructive example, namely the ferroelastic phase transition on arsenic pentoxide. A crystal of As_2O_5 has tetragonal symmetry at high temperatures (Salje, Bismayer & Jansen, 1987; Redfern & Salje 1988; Bismayer, Salje, Jansen & Dreher, 1986). This symmetry is reduced to orthorhombic in a ferroelastic phase with a characteristic change of lattice parameters from $a = b$ at $T > T_c$ to $b > a$ at $T < T_c$. The c lattice parameter is not directly involved in the transition mechanism (*i.e.* a shear motion occurs in the ab plane) and no equivalent variation of the c lattice parameter is observed. In order to evaluate the spontaneous strain, we have to extrapolate the lattice parameters of the high-symmetry phase into the temperature regime of the low-symmetry phase. This extrapolation represents that part of the thermal expansion which is not related to the structural phase transition and therefore does not contribute to the excess spontaneous strain. The numerical values of the spontaneous strain are now defined by the strain tensor which relates the low-symmetry unit cell to the high-symmetry unit cell when extrapolated to the same temperature.

In the case of arsenic pentoxide, the only non-zero components of the strain tensor are $e_{11} = -e_{22}$ which describe the expansion of the a axis and the equivalent contraction of the b axis. Note that, since these two effects compensate for each other, the volume of the unit cell does not change (in linear approximation). The numerical values of e_{11} and e_{22} are given by

$$e_{11} = -e_{22} = (b_{\text{orthorhombic}} - b_{\text{tetragonal}})/b_{\text{tetragonal}},$$

where the tetragonal lattice parameter is always the extrapolated value at the temperature at which the orthorhombic lattice parameter is measured, see Fig. 6(*a*). The resulting temperature evolution of the spontaneous strain is plotted in Fig. 6(*b*). It clearly shows the transition temperature as the point at which the spontaneous strain disappears with the crystal being paraelastic at higher temperatures and ferroelastic at

lower temperatures. By constructing the spontaneous strain we have reduced the total thermal expansion of the crystal to that part which is a true excess quantity (that is, it depends on the structural phase transition). The non-relevant background thermal expansion has been absorbed in the baseline in Fig. 6(*b*).

There are essentially three different ways in which the baseline can be derived from experimental observations.

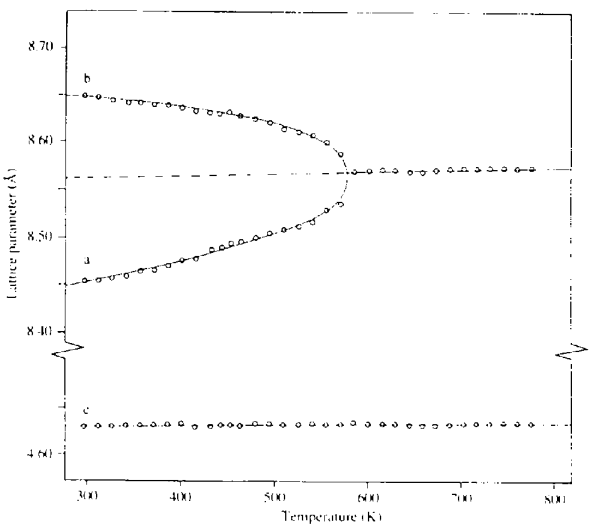

(*a*)

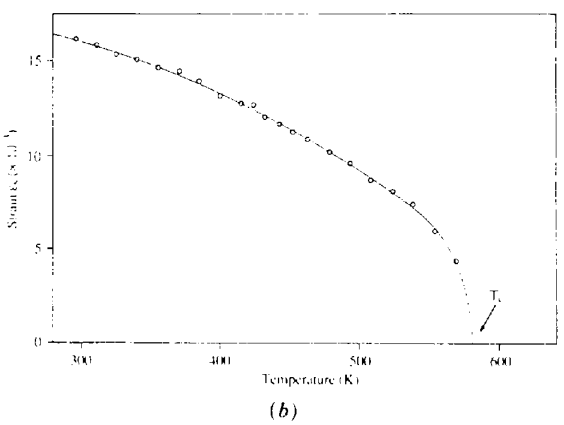

(*b*)

Fig. 6. (*a*) Temperature evolution of the lattice parameters in As_2O_5. The crystal has tetragonal symmetry at $T > T_c$ with $a = b$. At $T < T_c$ the symmetry reduces to orthorhombic $b > a$. The identical lattice parameters a and b in the high-symmetry phase can be extrapolated into the temperature interval of the low-symmetry phase (dotted line). The spontaneous strain is then related to the difference between the true lattice parameters (dotted line) which would have been obtained if the phase transition had not taken place. (*b*) Temperature dependence of the spontaneous strain as derived from the lattice parameters shown in Fig. 3(*a*). The line corresponds to the predicted behaviour of a second-order phase transition using Landau theory.

1. The lattice parameters are measured over a large temperature interval in the high-symmetry phase to warrant reliable extrapolation into the stability range of the low-symmetry phase.

2. The thermal expansion of the high-symmetry phase is ignored and the values of the lattice parameters closest to the transition point are used as temperature-independent reference values for all temperatures (*i.e.* the dotted reference line in Fig. 6(*a*) would be horizontal). This approximation might lead to systematic errors in the determination of the temperature evolution of the spontaneous strain, in particular if the numerical values of the spontaneous strain are small. A typical example which has largely been discussed in the literature is the $I\bar{1}$-$P\bar{1}$ phase transition in anorthite where the non-critical thermal expansion of the high-temperature phase is comparable in magnitude to the spontaneous strain arising from the phase transition (Redfern, Graeme-Barber & Salje, 1988). In most ferroelastic and co-elastic minerals with large spontaneous strains (say a few %), the systematic errors introduced by this procedure may be acceptable (Salje, 1990*a*).

3. The extrapolated lattice parameters of the high-symmetry phase in the phase field of the low-symmetry phase are constructed using some structural model. The most common one is to define an 'average' structure (Wadhawan, 1982). This structure is characterized by the arithmetic means of all possible strain tensors (*i.e.* for all domain orientations) in the low-symmetry phase. In arsenic pentoxide, for example, the two possible strain tensors are

$$e_{ik}(S1) = \begin{pmatrix} e_{11} & 0 & 0 \\ 0 & e_{22} & 0 \\ 0 & 0 & 0 \end{pmatrix}$$

and

$$e_{ik}(S2) = \begin{pmatrix} e_{22} & 0 & 0 \\ 0 & e_{11} & 0 \\ 0 & 0 & 0 \end{pmatrix}.$$

These two tensors represent two structural states in which the a and b axes are interchanged. The average structure is defined by the mean value

$$e_{ik}(\text{av.}) = \begin{pmatrix} \frac{1}{2}(e_{11}+e_{22}) & 0 & 0 \\ 0 & \frac{1}{2}(e_{11}+e_{22}) & 0 \\ 0 & 0 & 0 \end{pmatrix}.$$

The non-zero components of the latter tensor can now be expressed in lattice parameters, namely

$$\tfrac{1}{2}(e_{11}+e_{22}) = \tfrac{1}{2}[(a-a_0)/a_0 + (b-b_0)/b_0]$$

and with $a_0 = b_0$ in the tetragonal phase the condition that these tensor components vanish in the average structure (*i.e.* the hypothetical tetragonal structure at

low temperatures) becomes

$$a_0 = \tfrac{1}{2}(a+b).$$

Comparison with the experimental data in Figs. 6(*a*) and (*b*) shows that this approximation is indeed very good. The second advantage of this approximation is that similar relationships can easily be worked out for all experimental situations without any information about the lattice parameters of the high-symmetry phase at all.

The method has, on the other hand, a massive drawback. It is based on the assumption that the structural phase transition preserves the volume of the high-symmetry phase and that no other strain variations occur which are not fully described by the ferroelastic strain tensor (Aizu, 1970). This assumption is clearly wrong for most co-elastic materials where volume changes are often encountered (Salje, 1990*a*). More serious is the observation that sometimes even crystal structures which could reasonably be expected to be pure ferroelastics, such as leucite (Palmer, Salje & Schmahl, 1989; Boysen 1990), do indeed show strong volume anomalies. The construction of the spontaneous strain of leucite using the method of the average structure leads to a systematic error of almost 50% of the total spontaneous strain. These examples may illustrate that neither of these two approximations can be relied on without further detailed studies of the lattice parameters and, if possible, the thermal expansion of the crystallographic unit cell in the high-symmetry phase.

The spontaneous strain is a second-rank tensor, and the magnitudes of its components are hence not uniquely definable because they depend on the setting of the two crystallographic unit cells. For any given setting, however, the tensor components can be determined directly from the measured lattice parameters. In the following equations the lattice parameters of the low-symmetry phase are a, b, c, α, β, γ and those of the extrapolated high-symmetry phase are a_0, b_0, c_0, α_0, β_0, γ_0. The most general formulation for a triclinic system can be put into the form

$$e_{11} = a \sin\gamma / a_0 \sin\gamma_0 - 1$$

$$e_{22} = b/b_0 - 1$$

$$e_{33} = \frac{c \sin\alpha \sin\beta^*}{c_0 \sin\alpha_0 \sin\beta_0^*} - 1$$

$$e_{23} = \frac{1}{2}\left[\frac{c\cos\alpha}{c_0 \sin\alpha_0 \sin\beta_0^*} + \frac{\cos\beta_0^*}{\sin\beta_0^* \sin\gamma_0}\left(\frac{a\cos\gamma}{a_0} - \frac{b\cos\gamma_0}{b_0}\right) - \left(\frac{b\cos\alpha_0}{b_0 \sin\alpha_0 \sin\beta_0^*}\right)\right]$$

$$e_{13} = \frac{1}{2}\left(\frac{a\sin\gamma\cos\beta_0^*}{a_0 \sin\gamma_0 \sin\beta_0^*} - \frac{c\sin\alpha\cos\beta^*}{c_0 \sin\alpha_0 \sin\beta_0^*}\right)$$

$$e_{12} = \frac{1}{2}\left(\frac{a\cos\gamma}{a_0 \sin\gamma_0} - \frac{b\cos\gamma_0}{b_0 \sin\gamma_0}\right)$$

where the b axis has a common direction in both phases and the z direction in the Cartesian system of the strain tensor is parallel to $\mathbf{c}^*$ in the crystal (Redfern & Salje, 1987). Asterisks indicate values of the reciprocal-lattice parameters a^*, b^*, c^*, α^*, β^*, γ^* following the usual convention (see *e.g. International Tables for X-ray Crystallography*, 1969). Simplified expressions for higher-symmetry phases are listed by Salje (1990*a*) and can easily be used for the analysis of specific crystal systems.

For the definition of Aizu strains and the somewhat problematic use of the average structure as a reference state in the low-symmetry phase see Aizu (1970) and Wadhawan (1982).

Finally, it is convenient for a comparison of the degree of lattice distortion, described by the spontaneous strain in different systems, to define a scalar spontaneous strain $e_{\text{spontaneous}}$. The most common definition in the physical and crystallographic literature seems to be

$$e_{\text{spontaneous}} = e_s = (\sum e_i^2)^{1/2}$$

where e_i is the ith component of the spontaneous strain in the Voigt notation (although this definition is only a convenience to convert strain into a scalar quantity and is fairly arbitrary). Aizu (1970) used the tensor notation leading to the non-equivalent definition

$$e_{\text{Aizu}} = \left(\sum_{ik} e_{ik}^2\right)^{1/2}.$$

5. How the spontaneous strain and other structural parameters reflect the order parameter

The order parameter has been introduced as a purely thermodynamic quantity which describes the phase transition. The spontaneous strain and other crystallographic quantities such as occupancies, positional changes *etc.* reflect the order parameter and we must now ask how far the correlation between the thermodynamic and the structural parameters can be quantified. As an example, one finds that in some crystals the order parameter and the spontaneous strain are simply proportional to each other. In most crystals this is not the case, however, and one must explore the possible correlations rather carefully. The general scope of this treatment is the coupling theory (*e.g.* Salje & Devarajan 1986; Achiam & Imry, 1975; Gufan & Larin, 1980; Imry, 1975; Oleksy & Prysztawa, 1983). It is based on the assumption that the crystal is in thermodynamic equilibrium with a surrounding heat bath and that its structural state is

dictated by the condition that no structural variables can be changed without loss of energy. Here we shall also assume for the sake of simplicity that the crystal is homogeneous so that all fluctuation processes can be ignored (Salje, 1990*a*).

Here, the Gibbs free energy of a crystal with interacting Q and the spontaneous strain as one of the characteristic structural parameters can be formulated in three parts:

1. the thermodynamic energy directly related to the order parameter. In most structural phase transitions at high temperatures this part of the Gibbs free energy can be approximated by a Landau potential of the order parameter Q which we call $L(Q)$;
2. the elastic energy from the relaxation of the unit cell which is described by the spontaneous strain and the elastic constants of the paraelastic phase (*i.e.* the 'bare' elastic constants), $\frac{1}{2}\sum C_{ik}e_ie_k$ where C_{ik} are elastic constants, and;
3. the interaction energy between the order parameter Q and the spontaneous strain.

The Gibbs free energy can then be written as

$$G(Q, e) = L(Q) + \tfrac{1}{2}\sum_{ik} C_{ik}e_ie_k + \sum_{mn} \zeta_{i,m,n}e_i^m Q^n.$$

The last term represents the coupling energy in order n for the order parameter and in order m for the spontaneous strain ($n, m > 0$) ($\zeta_{i,m,n}$ are coupling constants between order parameters Q^n and strain elements). Just as for the order parameter Q and the spontaneous strain e_i, the coupling terms are subject to the constraints of symmetry and cannot be introduced arbitrarily. As a general rule, it holds that any combination of Q and e has to fulfil the same criteria to be a symmetry-allowed part of the Gibbs free energy as the higher-order polynomial terms in a Landau potential. If, for example, the symmetries of Q and e are identical, we find that all combinations $Q^ne_i^m$ with $n + m = p$ are allowed if Q^p is part of the Landau potential (this means in the language of group theory that Q and e_i transform according to the same irreducible representation).

Another general rule follows if e_i is a pure volume strain (*i.e.* it transforms as the identity representation). In this case we find that all coupling terms $n = 1$, $m > 1$ are symmetry allowed, where Q^m is part of the Landau potential.

The simplest case is the so-called bilinear coupling term Qe_i. If bilinear coupling is allowed by symmetry, it follows automatically that all higher-order couplings are also symmetry allowed. It was found by Devarajan & Salje (1984) that these higher-order terms may contribute significantly to the strain energy in sulfates and it is likely that similar effects occur in other framework structures so that higher-order coupling should not be automatically ignored even if bilinear coupling is compatible with symmetry (see also Hatch *et al.*, 1990).

No bilinear coupling can occur if the symmetry properties (*i.e.* the irreducible representations) of Q and e_i are different. The term which is always allowed by symmetry is $Q^2e_i^2$. This coupling term is called biquadratic. Further common coupling energies which have been observed in feldspars and langbeinites contain linear-quadratic, Q^2e_i, and linear-cubic, Q^3e_i, terms. There is as yet little experimental evidence that any coupling of orders higher than $m + n > 4$ provides a significant energy contribution and we restrict ourselves here to the discussion of the dominant bilinear and linear-quadratic coupling. The treatment of other coupling mechanisms is similar although analytically more strenuous [see Devarajan & Salje (1984) for a discussion of biquadratic coupling]. As an example, for higher-order strain coupling we refer to Rocquet & Couzi (1985) who discuss the case of $Na_5Al_3F_{14}$.

The correlation between the spontaneous strain and the order parameter for various orders leads not only to the possibility of following the temperature evolution of the order parameter *via* the measurements of lattice parameters but also correlates the derivatives of the Gibbs free energy with respect to the order parameter (*i.e.* the order-parameter susceptibility) with the equivalent derivative with respect to the strain. The latter quantity is equivalent to the elastic constants of the crystal which can be written as

$$C_{ik}^* = c_{ik} - \sum \frac{\partial^2 G}{\partial e_i\,\partial Q_m}\left(\frac{\partial^2 G}{\partial Q_m\,\partial Q_n}\right)^{-1}\frac{\partial^2 G}{\partial e_k\,\partial Q_n}$$

where e_i are the strain components and Q_n are the components of the order parameter. C_{ik} is the bare elastic constant which would occur if there were no phase transition. The consequences of this correlation for the elastic behaviour of the crystal was discussed in detail by Salje (1990*a*, and references cited therein). It is clear without further detailed analysis of this equation that any singularity of the susceptibility of the order parameter automatically leads to a softening of the elastic constants - a feature well documented in many experimental studies (review: Luti & Rehwald, 1981).

6. Coupling between different structural instabilities

It is an empirical observation that phase transitions in minerals and other materials of some complexity are often driven simultaneously by more than one physical mechanism. Typical examples are: the cation ordering of Al and Si in feldspars together with the atomic displacements involving the tilt of lattice complexes. Similarly, displacements interact with the molecular disorder in calcite, $NaNO_3$ (Dove, 1990; Schmahl & Salje, 1989; Harris, Salje & Güttler, 1990), and many other competitive interactions between different physical mechanisms leading to different

phase transitions have been reported [*e.g.* Flocken, Guenther, Hardy & Boyer (1985) on the competition between ferroelectricity and ferroelasticity; Toledano (1979) and Yoshihara, Yoshizawa, Yasuda & Fujimura (1985) on similar coupling in benzil]. If a crystal structure has sufficient complexity it will accommodate several of these structural instabilities with the outcome that the actual crystal structure is determined by a combination of all these transition mechanisms. The interaction between the ordering schemes often leads to seemingly complicated deformation patterns of crystal structures which do not appear to follow the theoretical predictions. The resulting crystal structures and their evolution with temperature, pressure *etc.* can, however, be greatly elucidated if we apply the same formal thermodynamic description to the structural properties as in the case of a phase transition with only one order parameter. In fact, each physical mechanism leading to a real or hypothetical phase transition has to be associated with a separate order parameter and the Gibbs free energy of the system must contain terms involving not only the individual order parameters but also terms to account for the effects of interactions, or coupling, between them.

As a knowledge of the effects of coupling between various order parameters with different physical meaning is essential for the understanding of complex materials, this point will be illustrated with the example of Na feldspar (Salje, 1985; Salje, Kuscholke, Wruck & Kroll, 1985) before we proceed with the formal description. The ferroelastic phase transition in Na feldspar, $NaAlSi_3O_8$, is illustrated in Fig. 7. At high temperatures ($T > 1251$ K), albite is monoclinic with space group C_2/m. On cooling, the symmetry is reduced to triclinic ($C\bar{1}$) by two interacting processes involving a displacive lattice distortion and the ordering of Al and Si atoms between the tetrahedral sites of the feldspar framework structure. The relevant order parameter of the Al, Si ordering is called Q_{od}. The displacive transition involves the rotation of the larger lattice complexes formed by a network of tetrahedra, the so-called crankshafts (Fig. 7). The parameter which describes this lattice distortion is called Q. Both transitions would result in the same symmetry change but the critical temperature of the displacive phase transition is 1251 K, in contrast to the lower transition temperature of the Al, Si ordering transition at *ca* 983 K. Each of these transition processes could occur independently if the other transition did not occur. If, for example, the displacive transition failed to occur, the Al, Si ordering transition would still take place. As the displacive transition in Na feldspar does occur, however, and reduces the symmetry to $C\bar{1}$ there is no further possibility for the Al, Si ordering to create an additional phase transition and the role of the Al, Si ordering is now limited to modifications of the displacive transition mechanism. These modifications are, nevertheless, essential and it is impossible to understand the physical behaviour of Na feldspar if either of these two transition mechanisms is ignored. Other examples for ferroelectric/ferroelastic coupling can be found in the excellent paper by Suzuki & Ishibashi (1987) and references given there.

6.1. *Coupling between two order parameters and the order-parameter vector space*

Let us first consider the simplest case of two interacting one-dimensional order parameters, both of which follow a simple Landau behaviour (extensions of the model can be treated in essentially the same way and do not contribute much to our understanding). In the case of Landau potentials with no odd-order terms we may write

$$G = \tfrac{1}{2}a_1Q_1^2 + \tfrac{1}{4}b_1Q_1^4 + \tfrac{1}{6}c_1Q_1^6 + \tfrac{1}{2}a_2Q_2^2 + \tfrac{1}{4}b_2Q_2^4 + \tfrac{1}{6}c_2Q_2^6 + \lambda_1Q_1Q_2 + \lambda_2Q_1^2Q_2^2.$$

Just as for order-parameter–strain coupling, the coupling terms are subject to the constraints of symmetry and cannot be introduced arbitrarily. Linear terms are excluded as they are excluded in the bare Landau potential and bilinear coupling is symmetry allowed if the transformation behaviour of Q_1Q_2 is the same as Q_1^2 or Q_2^2, *i.e.* the product representation contains

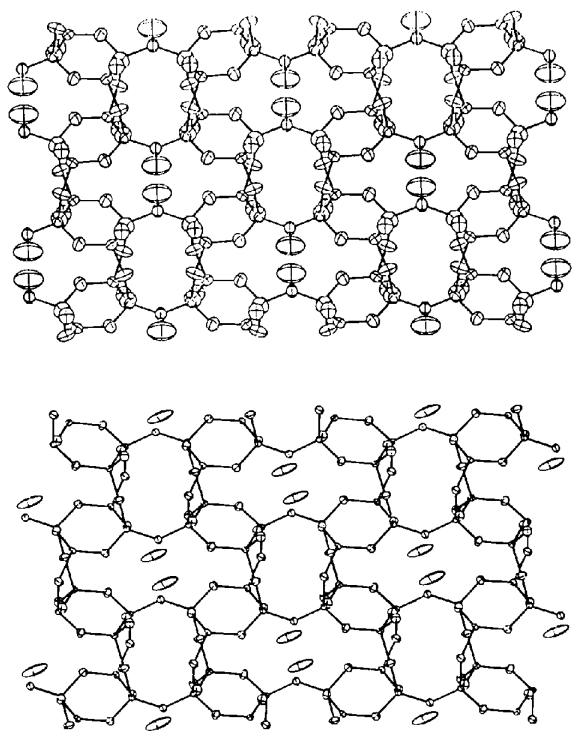

Fig. 7. Crystal structures of Na feldspar in the monoclinic phase (top) and the triclinic phase (bottom). During the phase transition, the mirror plane in the monoclinic structure is destroyed.

the identity representation if developed into irreducible representations. Even without going into the details of the group theoretical treatment, we can see immediately that bilinear coupling is compatible with symmetry if the symmetry properties of Q_1 and Q_2 are identical. In this case, all combinations Q_1^2, Q_2^2 and Q_1Q_2 have exactly the same symmetry constraints and they are all terms of the Landau potential. The behaviour of Na feldspar is a typical example for such a bilinear coupling. As the two order parameters Q and Q_{od} have the same symmetry behaviour and would individually lead to the same change of space group during the phase transition, the term QQ_{od} must also be a part of the Landau potential describing formally the coupling between Q and Q_{od}.

The second very common coupling scheme is represented by the biquadratic coupling $Q_1^2Q_2^2$. As both Q_1^2 and Q_2^2 are, by definition, part of the Landau potential, we find that their product will also be symmetry allowed. This leads to the important conclusion that biquadratic coupling always exists if a crystal structure relates to more than one order parameter. Uncoupled phase transitions are thus unphysical and may only appear in some approximation if the coupling energy is sufficiently small. The empirical evidence is, however, that coupling energies are normally not small at all in ferroelastic and coelastic crystals and that biquadratic coupling is a very common feature.

The remaining coupling energy of some importance is the linear–quadratic coupling in the form $Q_1Q_2^2$ which has to be invariant with respect to the active representation of the phase transition. The condition that a crystal is in thermodynamic equilibrium now requires that equilibrium is reached with respect to both order parameters. The Gibbs energy is thus an energy surface spanning a two-dimensional vector space with the basis vectors Q_1 and Q_2. The equilibrium point under given thermodynamic circumstances (*e.g.* at a given temperature) is a total minimum of the Gibbs energy in this order-parameter vector space:

$$\partial G/\partial Q_1 = 0, \qquad \partial G/\partial Q_2 = 0.$$

This treatment can obviously be expanded to order-parameter vector spaces with more than two interacting order parameters. Such situations are very common in nature (*e.g.* the above-mentioned case of Na feldspar) but no systematic exploration for higher dimensions than two have yet been undertaken.

We will now discuss the general topologies of the order-parameter vector spaces for the two most common coupling schemes, namely bilinear and biquadratic coupling. An equilibrium structural state which occurs under well defined temperature and pressure conditions represents one point in the order-parameter vector space as defined by the equilibrium condition. If the external conditions (*e.g.* T and P) are changed, we expect a different structural state to be more stable, which may or may not be related to the previous state in a continuous manner. Discontinuities can occur, however, only at points of first-order phase transitions but never inside the stability field of any phase or during a continuous phase transition. A further condition for bilinear coupling is that no single order parameter can disappear without the simultaneous disappearance of the second-order parameter. The only possible topology of the equilibrium line in the order-parameter vector space for bilinear coupling connects the origin ($Q_1 = Q_2 = 0$, *i.e.* the high-symmetry phase) with the solution at absolute zero temperature which can be normalized to $Q_1 = Q_2 = 1$. The experimental equilibrium line for Na feldspar is shown in Fig. 8 (Salje, Kuscholke, Wruck & Kroll, 1985).

Gufan & Larin (1980) were the first to point out that the intuitive assumption that similarly simple topologies also apply for higher-order coupling is wrong. Salje & Devarajan (1986) derived the seven possible topologies for biquadratic coupling which are displayed in Fig. 9. The three following conclusions can be drawn from visual inspection of these diagrams.

1. The stability range of the different phases may be changed and a succession of phase transitions may occur in place of a single phase transition. Such phase transitions occur each time the equilibrium line reaches the axes of the diagrams in Fig. 9. Cascades of phase transitions may occur if more order parameters couple. In particular, re-entrant phase transitions, where the same phase appears as a high- and low-temperature form with an intermediate phase with different symmetry, may result from biquadratic coupling.

2. The order of a phase transition is influenced by the coupling. As in the case of the order parameter – strain coupling, we find that a continuous phase transition can become discontinuous and *vice versa* due to the coupling energy.

3. The temperature evolution of the order parameter(s) near the transition point can be completely different from the expected simple Landau behaviour of one single order parameter. This does not, in general, indicate that the Landau approach is wrong but simply means that the interaction between order parameters has not been appreciated.

6.2. *Coupling via common strain components, a possible coupling mechanism*

The physical origin of order-parameter coupling can vary depending on the structural properties of the material under investigation. As long as we are interested in the thermodynamic description of the material, the different coupling mechanisms do not really matter because they will all be adequately

described by the Landau potential. The details of the phase-transition process are still universally related to the order parameters and the structural behaviour depends directly upon them. On the other hand, if we try to attach physical meaning to the various parameters in the Landau potential itself, we can gain confidence in the reliability of the coupling energies as determined indirectly from a thermodynamic treatment. It is, for example, normally expected that coupling energies describing the interaction between a spin-related order parameter and an order parameter correlated with a structural distortion will be small because we know that spin-phonon interactions contain relatively small amounts of energy (compared with phonon-phonon interactions). Cation ordering, on the other hand, will presumably couple strongly with lattice distortions, in particular if the cations involved have different sizes.

One specific coupling mechanism which appears to be a common feature is based on the elastic interactions between the two order parameters. Following the treatment of the order-parameter-strain coupling, each order parameter will create a spontaneous strain e_s. Let us now assume that the spontaneous strain created by either of the two order parameters has at least one common component e. We find that the

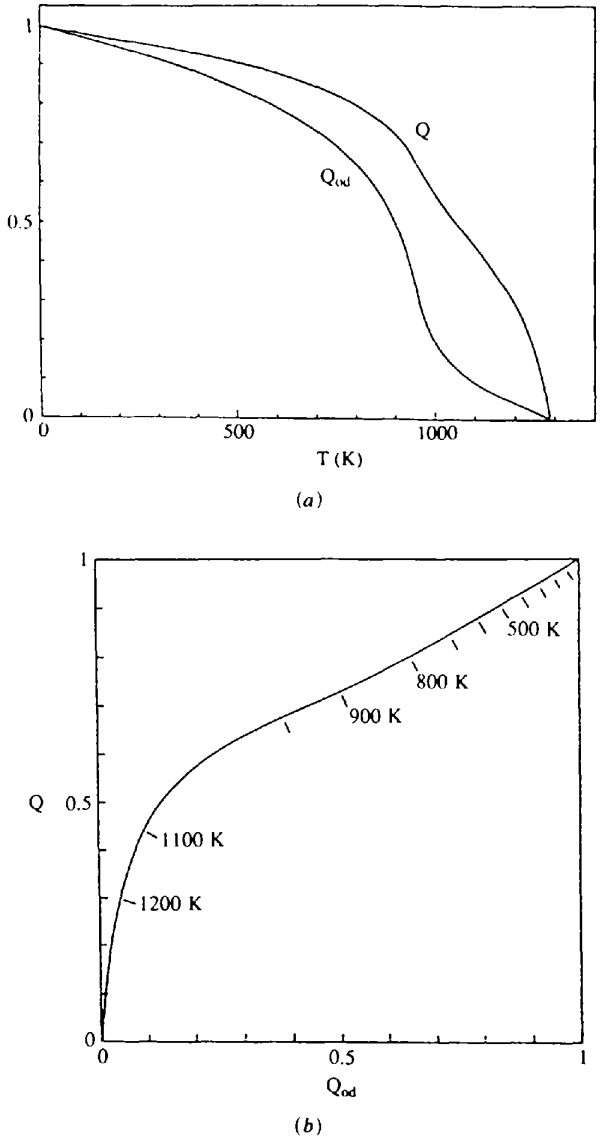

Fig. 8. (*a*) Temperature dependence of the 'displacive' order parameter Q and the Al, Si order parameter Q_{od} in thermodynamic equilibrium. (*b*) The same data as in (*a*) represented in the order-parameter vector space. The high-symmetry phase is represented by the origin and the most distorted structural state by the point $Q = Q_{od} = 1$ (from Salje *et al.*, 1985).

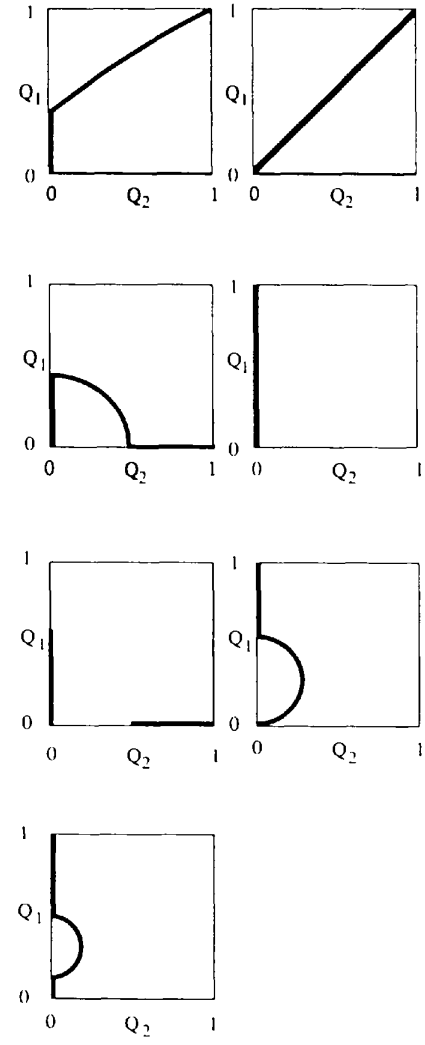

Fig. 9. Characteristic topologies of the order-parameter vector space for biquadratic coupling. The high-symmetry phase is the origin of all diagrams. Re-entrance phase transitions occur for 2-4-6 potentials (the numbers indicate the exponentials in the Landau potential).

Gibbs free energy

$$G(Q_1, Q_2, e) = \tfrac{1}{2}a_1Q_1^2 + \tfrac{1}{4}b_1Q_1^4 + \tfrac{1}{6}c_1Q_1^6 + \tfrac{1}{2}a_2Q_2^2 + \tfrac{1}{4}b_2Q_2^4 + \tfrac{1}{6}c_2Q_2^6 + d_1Q_1e + d_2Q_2e + \varepsilon_1Q_1^2e + \varepsilon_2Q_2^2e + fe^2$$

implicitly contains the coupling between the two order parameters. This coupling becomes obvious if we apply the condition that the crystal is free of strain:

$$\partial G/\partial e = 0$$

and find for $e_1 = e_2 = 0$

$$e = -(1/2f)(d_1Q_1 + d_2Q_2).$$

The Gibbs free energy is then

$$G = \tfrac{1}{2}(a_1 - d_1^2/2f)Q_1^2 + \tfrac{1}{4}b_1Q_1^4 + \tfrac{1}{6}c_1Q_1^6 + \tfrac{1}{2}(a_2 - d_2^2/2f)Q_2^2 + \tfrac{1}{4}b_2Q_2^4 + \tfrac{1}{6}c_2Q_2^6 - (d_1d_2/2f)Q_1Q_2.$$

This Landau potential is now identical with the original Gibbs free energy where the coupling terms are directly related to the elastic constants and to the magnitude of the spontaneous strain for the bilinear case and *via*

$$e = -(1/2f)(\varepsilon_1Q_1^2 + \varepsilon_2Q_1^2)$$

for the biquadratic coupling.

The correlation between the spontaneous strain, the elastic constants and the effective coupling constants shows clearly that a soft material with a large spontaneous strain will always be characterized by a strong coupling between the two order parameters, whereas a hard material with a small lattice distortion due to the phase transition is less susceptible to this coupling mechanism. As the elastic constants and the relevant strain components are normally known from experimental observations, it is always possible to estimate the coupling strength. The analytical solutions for bilinear and biquadratic coupling are given by Salje & Devarajan (1986) and examples are described by Salje (1990*a*).

7. Microstructures or 'we need a mesoscopic crystallography'

Crystal structures which are the result of structural phase transitions have so far been considered as homogeneous. A similar assumption (but using complex order parameters) also underlies the treatment of incommensurate and, more generally, modulated structures although the detailed treatment can be more involved than in the case of structures with well defined and relatively small translational periodicities. Other structures cannot easily be treated in the same way as homogeneous or quasi-homogeneous crystals. Such cases include nanocrystals and relaxor materials (Cross, 1987; Darlington, 1990; Salje & Bismayer, 1989), polaronic materials (Iguchi, 1991; Salje, 1990*b*; Mott, 1990) and all those crystals which underwent a ferroelastic or co-elastic phase transition under the formation of dense twin structures (Salje, 1990*a*). The largest group of such non-homogeneous structures are those which are created by kinetic processes, *e.g.* by rapid quench of the high-symmetry phase, which always leads to the formation of microstructures on a length scale which is larger than the interatomic distances but smaller than the macroscopic dimensions of the crystal. This mesoscopic length scale is often of the order of 100 Å and well within the realm of transmission electron microscopy. Classical crystallographic methods of X-ray and neutron diffraction, on the other hand, are not easily employed on this length scale and it appears that much of what can be predicted theoretically has, in fact, not yet been manifested on a firm experimental basis. Some of the important points are the bending of lattice planes in the vicinity of twin boundaries, the fine structure of tweed microstructures and the transport of solitonic and solitary excitations. Some recent progress in this field of 'mesoscopic' crystallography has been reviewed by Salje (1990*a*). In this paper the structural phase transition in the high-temperature superconductor $YBa_2Cu_3O_{7-\delta}$ is considered as an example of a crystal in which the microstructural features on a length scale large compared with the interatomic distances are relevant for the understanding of the phase transition.

The routine synthesis of the superconducting phase of $YBa_2Cu_3O_7$ is by supercooling an oxygen-deficient phase ($\delta \simeq 0{\cdot}1$) leading to a tetragonal phase ($P4/mmm$). This precursor material is then annealed in oxygen and cooled through a phase transition to the orthorhombic phase ($Pmmm$). Twinning in {110} occurs as a consequence of the ferroelastic phase transition with a spontaneous strain $e = 2(a-b)/(a+b)$, with reported domain sizes ranging from 10^{-10} to 10^{-4} M (Fig. 10). An understanding of

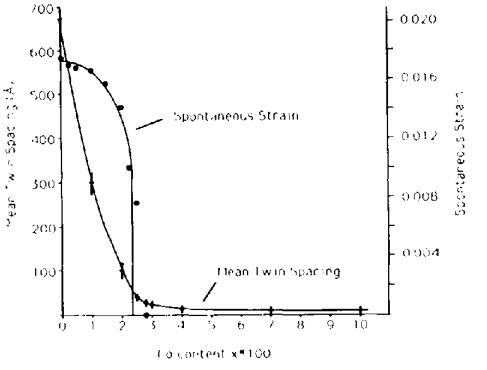

Fig. 10. Spontaneous strain and mean twin spacing in the high-temperature superconductor $YBa_2Cu_3O_7$:Co. The phase transition is obtained by chemical replacement of Cu by Co.

the effect of the twin microstructure is important for the superconducting performance because the twin walls can act as pinning centres (Chaudhari, 1987) and are sometimes considered as weak links which may act as Josephson junctions (Deutscher & Müller 1987).

In Fig. 11 the average structure of the precursor material is shown (Schmahl, Salje & Liang 1988). The phase transition is driven mainly by the ordering of the oxygen vacancies in the O(1) sites while the O(2) sites remain partly occupied in both the orthorhombic and tetragonal phases (Schmahl *et al.*, 1988; Jorgensen *et al.*, 1987). Besides the ordering process of the vacancies we find that the thermodynamic order parameter of the structural phase transition must also be correlated with the spontaneous strain and the dominant relaxations of the atomic positions. The atomic shifts due to the phase transition are

(1) the Ba positions moving towards the 'soft' Cu(1)–O layer as the oxygen content increases; and

(2) the Cu(1)–O(2) distances increase when more Cu(1)–O(2) bonds are formed. Simultaneously,

(3) the Cu(2)–O(2) distances decrease and

(4) Cu(2) moves out of the O(3) square towards O(2);

(5) the Cu(1)–Cu(2) distances bridged by O(2) decrease and

(6) the non-bridged Cu(2)–Cu(2) contact along the *c* axis increases.

The total deformation pattern is shown in Fig. 12 (after Schmahl *et al.*, 1988).

The atomic movements, the ordering pattern of oxygen and the spontaneous strain follow the transformation pattern of the B_{1g} irreducible representation. In the tradition of the Landau theory of structural phase transitions the elastic energy is usually singled out as part of the excess Gibbs free energy. This is justified because of the long-range character of the spontaneous strain which leads to a mean-field behaviour of the transition mechanism even when the local displacements and occupancies might suggest an iso-spin behaviour (Marais, Heine & Salje 1991). A further important variable in $YBa_2Cu_3O_{7-\delta}$ is the amount of dopants, such as Co, Fe or Zn. The total Gibbs free energy related to the phase transition was approximated by Schmahl *et al.* (1988) as

$$\begin{aligned} G(\eta, Q, e) = G_0 &+ \tfrac{1}{2}k_B T[(1-\eta)\ln(1-\eta) \\ &+ (1+\eta)\ln(1+\eta)] \\ &+ \tfrac{1}{2}(1-\eta^2)k_B T_\eta(1+\mu_{el}e+\mu_Q Q+\dots) \\ &+ \tfrac{1}{2}a(T-T_Q)Q^2+\tfrac{1}{4}bQ^4+\tfrac{1}{6}cQ^6+\dots \\ &+ \lambda Qe+fe^2\dots \\ &+ \sum g_\eta(\nabla\eta)^2+\sum g_Q(\nabla Q)^2+\sum g_e(\nabla e)^2 \\ &+ \sum g_{\eta e}(\eta\nabla e)+\sum g_{\eta Q}(\eta\nabla Q) \\ &+ \sum g_{eQ}(e\nabla Q)+\sum g_{Qe}(Q\nabla e)+\dots . \end{aligned}$$

The minimum of this energy expression determines the structural state at any temperature, chemical composition and amount of doping.

So far the structural phase transition has been treated as an equilibrium phenomenon. The question arises, however, as to whether the crystal as observed in the actual experiment represents a thermodynamic equilibrium state (Salje, 1989). The answer depends to a large extent on structural properties (and their related energies) which extend over a mesoscopic scale rather than being measured on an atomistic level. A well known example of a simple nonequilibrium feature is twin structures (Fig. 13). In a hypothetical crystal with harmonic interactions between the atoms (*e.g.* a ball-and-spring model of an NaCl structure), a low-symmetry phase can be thought of as a pure shear of the high-symmetry form. Twin walls will form which contain no excess Gibbs free energy provided the compatibility relationship between each pair of adjacent domains is met (Salje, 1990*a*; Sapriel, 1975; Marais *et al.*, 1991; Barsch & Krumhansl, 1988). In the real crystal, this approximation is inappropriate because local displacements, ordering *etc.* create structural strain fields in and close to the wall. The fine structure of the wall changes due to these local relaxations from bicrystals to kink solitary excitations (Fig. 14). As a consequence of these excitations one observes typical geometrical configurations which allow a description of microstructures in crystallographic terms. Typical examples are the following. In the case of parallel walls, effective wall-wall interactions lead to periodic wall

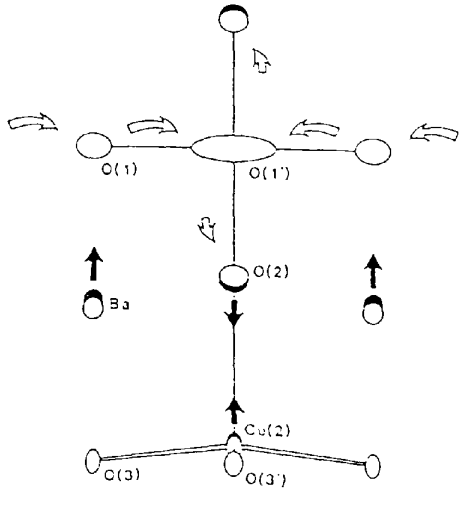

Fig. 12. Deformation pattern of the tetragonal-orthorhombic phase transition in $YBa_2Cu_3O_{7-\delta}$. Open ellipsoids represent the positions in the low-symmetry phase, the full ellipsoids those in the high-symmetry phase. The straight arrows indicate the directions of the atomic displacements, the curved arrows symbolize the oxygen transport.

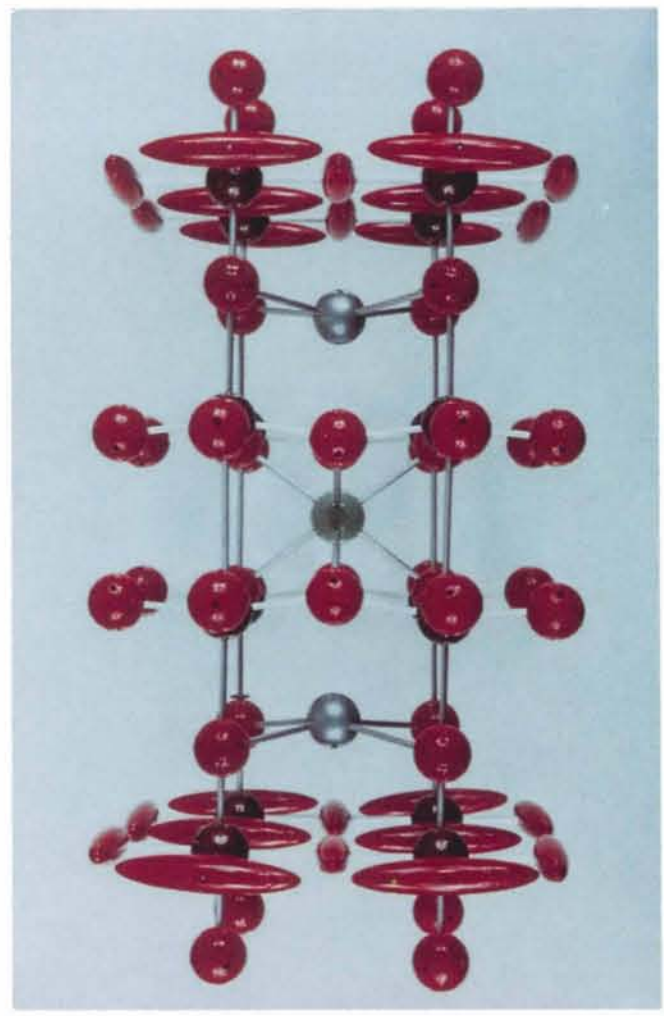

Fig. 11. Average structure of tetragonal $YBa_2Cu_3O_{6\cdot45}$. Note the larger probability ellipsoids of the O-atom positions in the soft Cu(1) layer at the top and at the bottom of the structure.

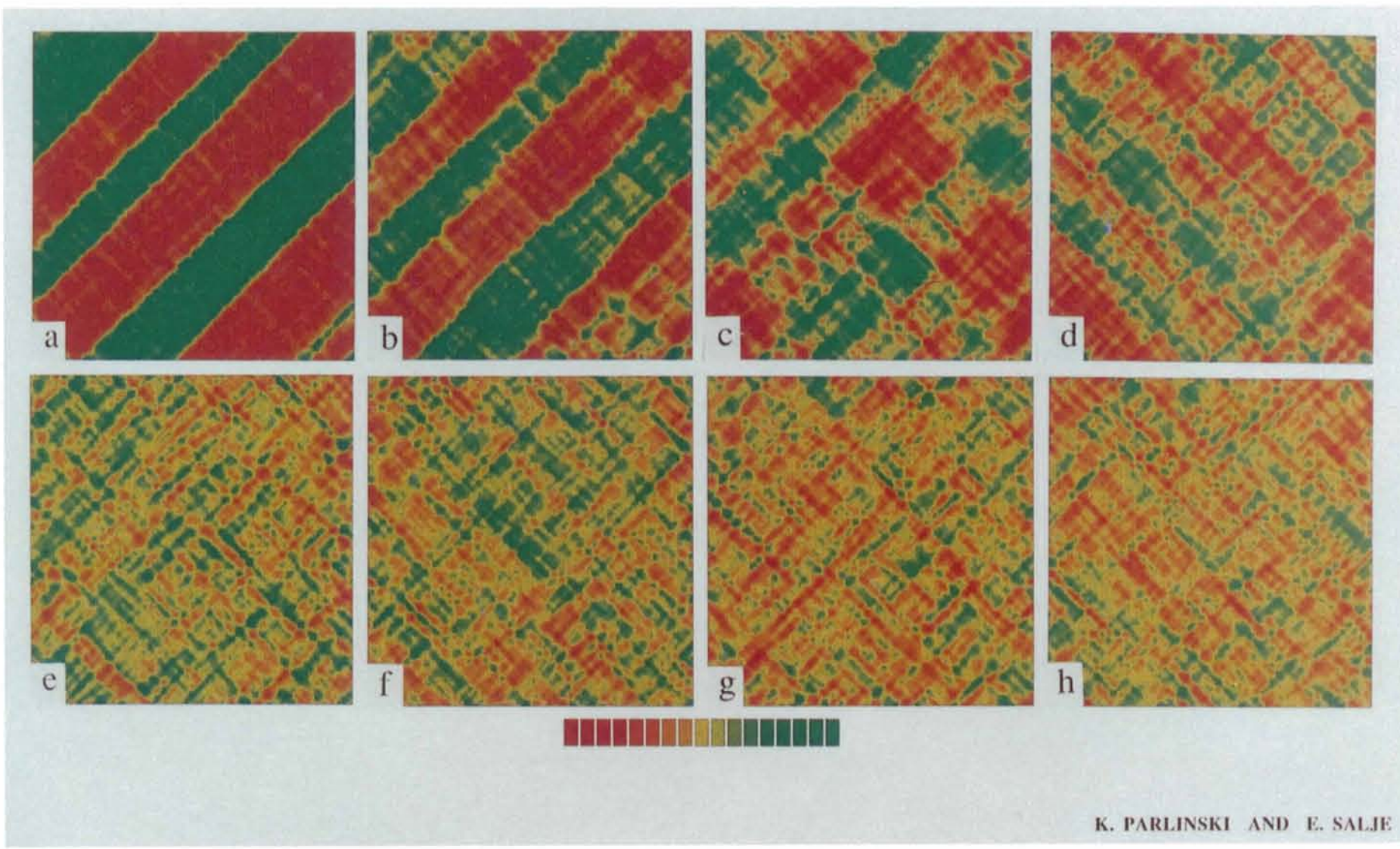

Fig. 16. Map of the strain distribution obtained by computer simulation. The colour scale is adjusted to the local orthorhombic lattice distortion. Red and green correspond to the two possible orientations of the orthorhombic unit cell. Yellow denotes the undistorted tetragonal unit cells. Maps (*a*), (*b*), (*c*) and (*d*) have been obtained under fast cooling to 0·67×, 0·83×, 0·86× and 0·93 × T_c. Maps (*e*), (*f*), (*g*) and (*h*) correspond to slow heating at 1·1×, 1·16×, 1·37× and 1·59 × T_c where T_c is the transition temperature.

[*to face page* 466

patterns in a similar way as periodic patterns with large repetition units are found in polytypic materials (Cheng, Heine & Jones, 1990; Winkler, Dove, Salje, Leslie & Palosz, 1991). Intersecting walls lead to positive energy singularities at the junctions which are strong enough to bend the lattice plane around the intersections (Salje, Kuscholke & Wruck, 1985). Other geometrical wall patterns related to transformation twinning are described in detail by Salje (1990*a*) and the references given there.

So far we have seen that twin walls represent non-equilibrium features because the untwinned crystal (without boundary constraints) has a lower Gibbs free energy than the twinned crystal. The associated structural distortions are relatively small when related to the bulk of the material. Much larger excess Gibbs free energies related to such mesoscopic structures are encountered if the crystal has created the microstructure *via* a kinetic process. In experimental terms, this might occur when a crystal is quenched or shock heated so that the order parameter is no longer in thermodynamic equilibrium. The subsequent structural relaxation will then lead to variations of the order parameter which can no longer be described as a small perturbation from an equilibrium situation. The time evolution in the case of smooth energy surfaces can be approximated by (Salje, 1988; Dattagupta, Heine, Marais & Salje, 1991)

$$\frac{\partial Q(x)}{\partial t} = \frac{\gamma\langle a^2\rangle}{2k_B T}\left[1 - \frac{\xi_c^2}{\xi^2}\frac{\sinh(\xi\nabla)}{\xi\nabla}\right]\frac{\partial G}{\partial Q(x)}$$

where γ is the Onsager coefficient, a is a characteristic length related to the structural dimensions, G is the excess Gibbs energy which is reduced during the kinetic process, ξ_c is the characteristic length scale which determines whether the order parameter is conserved ($\xi = \xi_c$) or non-conserved ($\xi_c = 0$). This rate law can be directly derived as a mean-field approximation from a combined Glauber–Kawasaki master equation. Let us now consider the influence of fluctuations which change the microstructure of the crystal. The simplest case is $\xi_c = 0$ (*i.e.* a non-conserved order parameter) and a parabolic Gibbs free energy $dG/dQ = \chi^{-1}Q$. The noise is represented by the distribution function $P(\chi^{-1})$ so that the mean order parameter, averaged over the volume, becomes

$$\langle Q\rangle = L(P) = \int_0^x P(x)\exp(-xt)\,dx.$$

This rate law is significantly different from a simple exponential decay which would occur if the crystal

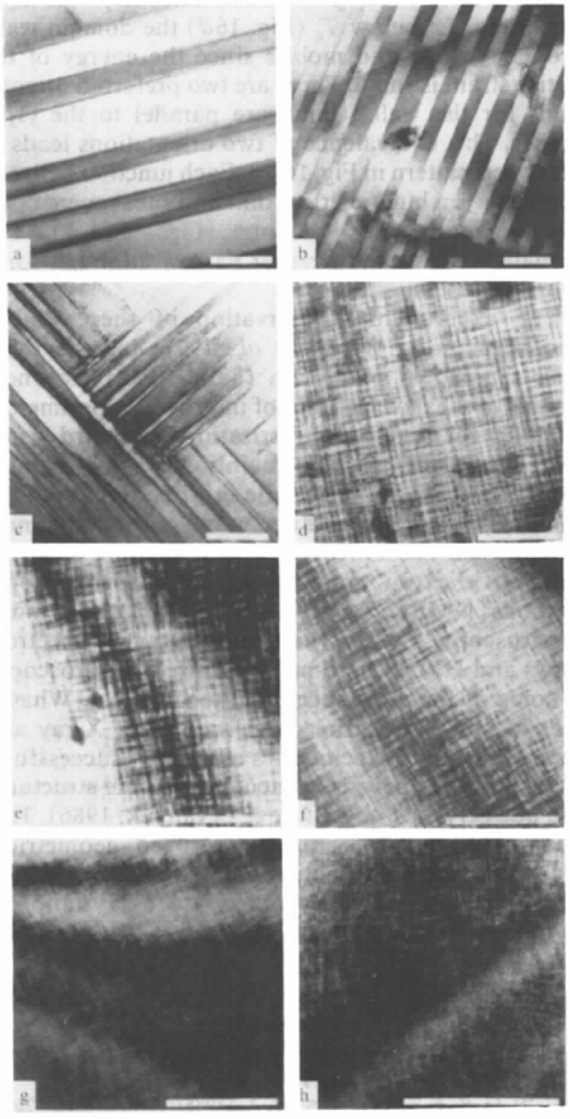

Fig. 13. Transmission electron micrographs of Co-doped $YBa_2Cu_3O_7$ with the incident beam along [001]. Length of scale bar: 0·1 μm, compositions from (*a*) to (*h*): 0·0, 0·01, 0·02, 0·025, 0·028, 0·03, 0·04 and 0·07 Co for Cu.

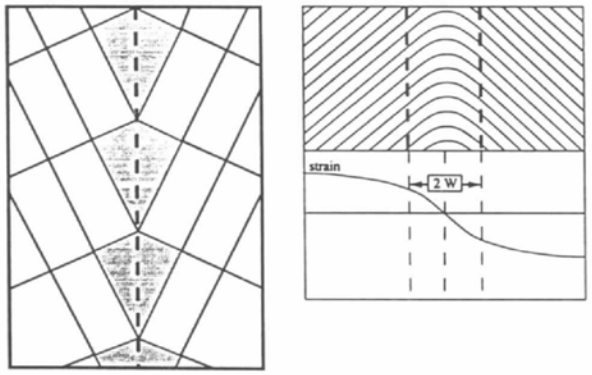

Fig. 14. Bicrystal configuration for a twin wall (left) and kink soliton solution in an elastic continuum (W indicates the solitonic wall thickness).

were free of noise. As a consequence of the distribution in Q the crystal must become spatially inhomogeneous. This inhomogeneity is often related to strain effects which develop on a length scale of some 100 Å. Salje & Wruck (1988) have undertaken model calculations in which they found wide distributions of the order parameter even when the initial starting material and the final annealing product were perfect single crystals, experimental evidence for the predicted kinetic tweed structure was found by Wruck, Salje & Graeme-Barber (1991). It was also predicted that, in the case of a white-noise spectrum, the crystals develop glass-like states for intermediate kinetic structures. These microstructures disappear with increasing annealing time when the crystal approaches thermodynamic equilibrium.

Similar progress has been made for the calculation of microstructures using simple models describing interatomic forces (Parlinski, 1988). As an example, let us consider a layer structure such as $YBa_2Cu_3O_7$ (Salje & Parlinski, 1991). The various forces are depicted as springs in Fig. 15. The phase transition is driven by the occupancy of oxygen at positions z_1 and z_2 (black circles). This occupancy is modelled using a local potential with two minima, one minimum represents the occupied state, the other minimum represents the empty state. The total Hamiltonian is then of the same type as discussed in § 2 of this paper:

$$H = \tfrac{1}{2}\sum_m \nu_m^2 + \tfrac{1}{2}\sum_l \nu_l^2 + \tfrac{1}{2}\sum_{n,n} A(R_{m,m'} - a_0 - \alpha z_i)^2 + \sum_{(n,n,n)} B(R_{m,m'} - a - \sqrt{2})^2 + \sum_{ll} J_{ij} z_i z_j + \sum_l (Ez_l^2 + Gz_l^4)$$

where ν_m and ν_l are the velocities of atoms (Cu and O), $R_{m,m'}$ is the distance between Cu atoms m and m', a_0 is the high-temperature lattice constant and z_i represents the state of the oxygen position. The summation runs over all Cu atoms (n), nearest neighbours (n, n), next-nearest neighbours (n, n, n), oxygen atoms (l) and their nearest neighbours (l, l). The model was calculated using molecular dynamics techniques on 99×99 unit cells with the kinetic energy of the system taken as a measure of the temperature. Microstructures occur as a result of rapid changes of temperatures. In Fig. 16 the results of such 'quench experiments' are shown. The colours represent the local strain fields with red and green as the positive and negative spontaneous strain. The yellow areas are the undistorted parts of the crystal structure. In Figs. 16(e)-(h), the crystal is in the high-symmetry phase although locally distorted regions still exist for temperatures well above the transition point. Maps (a)-(d) of Fig. 16 have been obtained under fast cooling. The cooling rate was sufficiently fast to allow many domains to grow simultaneously. At temperatures just below T_c (Fig. 16d) the domain walls are very rough and mobile since the energy of the lattice strain is small. There are two preferred orientations for the walls which are parallel to the $\langle 1, 1\rangle$ planes. This equivalence of two orientations leads to the tweed pattern in Fig. 16(c). Each junction between two walls is a high-energy point and subsequent cooling eradicates the junctions (Figs. 16a, b). The domain walls are now rather narrow although some roughness persists.

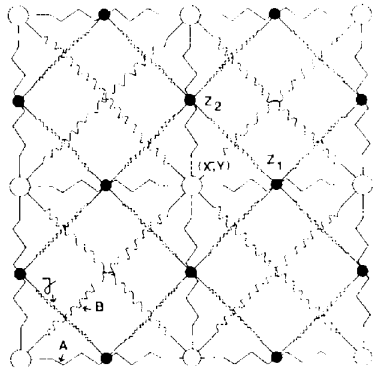

Fig. 15. Two-dimensional model used in the molecular dynamics simulations.

The experimental observation of these kinetic microstructures (Wruck *et al.*, 1991) together with their theoretical prediction (Salje, 1988) may now lead us to the development of improved experimental facilities for their characterization. Standard structural analytical methods mainly solve the average structure which contains little information about the correlations within the fluctuations. So far the most reliable analysis relies on a combination of transmission electron microscopy and spectroscopic methods [NMR, EXAFS, XANES, optical hard mode spectroscopy, HMRS (hard mode Raman spectroscopy) and HMIS (hard mode infrared spectroscopy) as some of the most successful techniques]. What is needed now is a further development of X-ray and neutron scattering techniques as already successfully applied to the analysis of incommensurate structures and quasicrystals (*e.g.* Blinc & Levanyuk, 1986). This would lead us to a much improved geometrical characterization of fluctuation pattern and related microstructures and - ultimately - to a crystallography of the mesoscopic length scale.

References

ACHIAM, Y. & IMRY, Y. (1975). *Phys. Rev. B*, **12**, 2768-2776.
AIZU, K. (1970). *J. Phys. Jpn.* **28**(3), 706-716.
BARSCH, G. R. & KRUMHANSL, J. A. (1988). *Acta Metall. Trans.* A19A, 761-775.
BISMAYER, U., SALJE, E., JANSEN, M. & DREHER, S. (1986). *J. Phys. C*, **19**, 4537-4545.
BLINC, R. & LEVANYUK, A. P. (1986). *Mod. Probl. Condens. Matter Sci.* **14**.

BOYSEN, H. (1990). In *Phase Transitions in Ferroelastic and Co-elastic Crystals*, edited by E. K. H. SALJE, pp. 320-335. Cambridge Univ. Press.
BRUCE, A. D. & COWLEY, R. A. (1981). *Structural Phase Transitions*. London: Taylor & Francis.
CHAUDHARI, P. (1987). *Jpn. J. Appl. Phys.* **26**, 2023-2034.
CHENG, C., HEINE, V. & JONES, I. L. (1990). *J. Phys. Condens. Matter*, **2**, 5097-5114.
CROSS, L. E. (1987). *Ferroelectrics*, **76**, 241-267.
DARLINGTON, C. N. W. (1990). In *Phase Transitions in Ferroelastic and Co-elastic Crystals*, edited by E. K. H. SALJE, pp. 270-282. Cambridge Univ. Press.
DATTAGUPTA, S., HEINE, V., MARAIS, S. & SALJE, E. (1991). *J. Phys. Condens. Matter*. In the press.
DEUTSCHER, G. & MÜLLER, K. A. (1987). *Phys. Rev. Lett.* **59**, 1745-1747.
DEVARAJAN, V. & SALJE, E. (1984). *J. Phys. C*, **17**, 5525-5537.
DOVE, M. T. (1990). In *Phase Transitions in Ferroelastic and Co-elastic Crystals*, edited by E. K. H. SALJE, pp. 297-311. Cambridge Univ. Press.
FLOCKEN, J. W., GUENTHER, R. A., HARDY, J. R. & BOYER, L. L. (1985). *Phys. Rev. B*, **31**, 7252-7260.
GUFAN, YU. M. & LARIN, E. S. (1980). *Sov. Phys. Solid State*, **22**, 270-273.
HARRIS, M. J., SALJE, E. K. H. & GÜTTLER, B. K. (1990). *J. Phys. Condens. Matter*, **2**, 5517-5527.
HATCH, D. M., ARTMAN, J. I. & BOERIO-GOATES, J. (1990). *Phys. Chem. Miner.* **17**, 334-343.
IGUCHI, E. (1991). *Solid State Chem.* In the press.
IMRY, Y. (1975). *J. Phys. C*, **8**, 567-577.
International Tables for X-ray Crystallography (1969). Vol. I. Birmingham: Kynoch Press.
ISHIBASHI, Y., HARA, K. & SAWADA, A. (1988). *Physica (Utrecht)*, **B150**, 258-264.
JORGENSEN, J. D., VEAL, B. W., KWOK, W. K., CRABTREE, G. W., UMEZAWA, A., NOWICKI, L. J. & PAULIKAS, A. P. (1987). *Phys. Rev. B*, **36**, 5731-5734.
LUTI, B. & REHWALD, W. (1981). *Curr. Phys.* **23**, 131-184.
LYNDEN-BELL, R. M., FERRARIO, M., MCDONALD, I. R. & SALJE, E. (1989). *J. Phys. Condens. Matter*, **1**, 6523-6542.
MARAIS, S., HEINE, V. & SALJE, E. (1991). In preparation.
MOTT, N. F. (1990). *Adv. Phys.* **39**, 55-81.
OLESKY, C. & PRYSZTAWA, J. (1983). *Physica (Ultrecht)*, **121A**, 145-149.
PALMER, D. C., SALJE, E. K. H. & SCHMAHL, W. W. (1989). *Phys. Chem. Miner.* **16**, 714-719.
PARLINSKI, K. (1988). *Comp. Phys. Rep.* **8**, 157.
REDFERN, S. A. T., GRAEME-BARBER, A. & SALJE, E. (1988). *Phys. Chem. Miner.* **16**, 157-163.
REDFERN, S. A. T. & SALJE, E. (1987). *Phys. Chem. Miner.* **14**, 189-195.
REDFERN, S. A. T. & SALJE, E. (1988). *J. Phys. C*, **21**, 277-285.
ROCQUET, P. & COUZI, M. (1985). *J. Phys. C*, **18**, 6571-6579.
SALJE, E. (1985). *Phys. Chem. Miner.* **12**, 93-98.
SALJE, E. (1988). *Phys. Chem. Miner.* **15**, 336-348.
SALJE, E. (1989). *Philos. Mag. Lett.* **59**, 219-221.
SALJE, E. (1989). *Philos. Trans. R. Soc. London Ser. A*, **328**, 409-416.
SALJE, E. K. H. (1990*a*). Editor. *Phase Transitions in Ferroelastic and Co-elastic Crystals*. Cambridge Univ. Press.
SALJE, E. (1990*b*). *Philos. Mag. Lett.* **62**, 277-282.
SALJE, E. & BISMAYER, U. (1989). *J. Phys. Condens. Matter*, **1**, 6967-6976.
SALJE, E., BISMAYER, U. & JANSEN, M. (1987). *J. Phys. C*, **20**, 3613-3620.
SALJE, E. & DEVARAJAN, V. (1986). *Phase Transitions*, **6**, 235-248.
SALJE, E., KUSCHOLKE, B. & WRUCK, B. (1985). *Phys. Chem. Miner.* **12**, 132-140.
SALJE, E., KUSCHOLKE, B., WRUCK, B. & KROLL, H. (1985). *Phys. Chem. Miner.* **12**, 99-107.
SALJE, E. & PARLINSKI, K. (1991). *Superconductor Science and Technology*. In the press.
SALJE, E. & WRUCK, B. (1988). *Phys. Chem. Miner.* **16**, 140-147.
SALJE, E. K. H., WRUCK, B. & THOMAS, H. (1991). *Z. Phys.* **B82**, 399-404.
SAPRIEL, J. (1975). *Phys. Rev. B*, **12**, 5128-5140.
SCHMAHL, W. W. & SALJE, E. (1989). *Phys. Chem. Miner.* **16**, 790-796.
SCHMAHL, W. W., SALJE, E. & LIANG, W. Y. (1988). *Philos. Mag. Lett.* **58**, 173-181.
STOKES, H. T. & HATCH, D. M. (1988). *Isotropy Subgroups of the 230 Crystallographic Space Groups*. Singapore: World Scientific.
SUZUKI, T. & ISHIBASHI, Y. (1987). *J. Phys. Soc. Jpn*, **56**, 596-602.
TOLEDANO, J. C. (1979). *Phys. Rev. B*, **20**, 1147-1156.
TOLEDANO, J. C. & TOLEDANO, P. (1980). *Phys. Rev. B*, **21**, 1139-1172.
TOLEDANO, J. C. & TOLEDANO, P. (1982). *Phys. Rev. B*, **25**, 1946-1964.
WADHAWAN, V. K. (1982). *Phase Transitions*, **3**, 3-103.
WINKLER, B., DOVE, M. T., SALJE, E. K. H., LESLIE, M. & PALOSZ, B. (1991). *J. Phys. Condens. Matter*. Submitted.
WRUCK, B., SALJE, E. & GRAEME-BARBER, A. (1991). *Phys. Chem. Miner.* In the press.
YOSHIHARA, A., YOSHIZAWA, M., YASUDA, H. & FUJIMURA, T. (1985). *Jpn. J. Appl. Phys. Suppl.* **24**, 367-369.

Acta Cryst. (1991). A**47**, 469-480

Derivation of Exponential Joint Probability Distributions of Structure Factors in *P*1 with Maximum Entropy and Irreducible Cluster Integrals

BY M. J. KRONENBURG, R. PESCHAR AND H. SCHENK

Laboratory for Crystallography, University of Amsterdam, Nieuwe Achtergracht 166, 1018 *WV Amsterdam, The Netherlands*

(*Received* 10 *October* 1990; *accepted* 7 *May* 1991)

Abstract

Recently the application of the maximum-entropy method to direct methods has been initiated for *a priori* uniformly and independently distributed atoms, introducing non-uniformity in direct space by putting constraints on the expected values of the distribution [Bricogne (1984). *Acta Cryst.* A**40**, 410-

0108-7673/91/050469-12$03.00